New constraints on crustal structure in eastern Afar from the analysis of receiver functions and surface wave dispersion in Djibouti

MULUGETA T. DUGDA & ANDREW A. NYBLADE

Department of Geosciences, Penn State University, University Park, PA USA 16802 (e-mail: mulugeta@geosc.psu.edu; andy@geosc.psu.edu)

Abstract: Crustal structure beneath the GEOSCOPE station ATD in Djibouti has been investigated using $H-\kappa$ stacking of receiver functions and a joint inversion of receiver functions and surface wave group velocities. We obtain consistent results from the two methods. The crust is characterized by a Moho depth of 23 ± 1.5 km, a Poisson's ratio of 0.31 ± 0.02, and a mean V_p of *c.* 6.2 km s^{-1} but *c.* 6.9–7.0 km s^{-1} below a 2–5 km-thick low-velocity layer at the surface. Some previous studies of crustal structure for Djibouti placed the Moho at 8 to 10 km depth, and we attribute this difference to how the Moho is defined (an increase of V_p to 7.4 km s^{-1} in this study vs. 6.9 km s^{-1} in previous studies). The crustal structure we obtained for ATD is similar to crustal structure in many other parts of central and eastern Afar. The high Poisson's ratio and V_p throughout most of the crust indicate a mafic composition and are not consistent with models invoking crustal formation by stretching of pre-existing Precambrian crust. Instead, we suggest that the crust in Afar consists predominantly of new igneous rock emplaced during the late syn-rift stage where extension is accommodated within magmatic segments by dyking. Sill formation and underplating probably accompany the dyking to produce the new and largely mafic crust.

Afar is a tectonically active region in between continental rifting and oceanic rifting where the Red Sea oceanic ridge, the Gulf of Aden oceanic ridge, and the continental East African Rift System (EARS) meet in a rift–rift–rift triple junction (Fig. 1). Understanding the nature and origin of the crust in Afar is important because Afar is one of the few places where it is possible to study the development of magmatic segmentation during rifting, the formation of volcanic rifted margins, and more generally, how continental rifts evolve into oceanic rifts.

There are a number of conflicting views about the thickness and composition of the crust in Afar, and how it formed. For example, some studies have reported estimates of crustal thickness between 14 and 26 km, and from these estimates inferred that the crust may be more continental than oceanic in nature (Makris & Ginzburg 1987; Berkhemer *et al.* 1975). Other studies have reported estimates of crustal thickness between 8 and 10 km (Ruegg 1975; Sandvol *et al.* 1998), suggesting an oceanic origin for the crust, and yet others have argued for completely new igneous crust that is much thicker than typical oceanic crust based on such observations as the velocity structure of the crust and Poisson's ratio (Mohr 1989; Dugda *et al.* 2005).

In this paper, crustal structure is imaged beneath the GEOSCOPE station ATD in eastern Afar (Djibouti) using receiver functions and surface wave dispersion measurements. We report new estimates of Moho depth, Poisson's ratio and shear velocity structure, and combine these estimates with seismic images of crustal structure from other parts of Afar to re-examine the nature and origin of the crust in Afar. This study differs from previous studies of receiver functions for station ATD in that 10 years of data have been used, enabling us to obtain high-quality receiver function stacks and to investigate azimuthal variations in structure beneath the station. In addition, Rayleigh wave group velocities have been used to constrain crustal shear wave velocities.

Tectonic and geodynamic setting

The seismic station ATD is located on the south side of the Gulf of Tadjoura in Djibouti (Figs 1 and 2). The Gulf of Tadjoura is the western extension of the Gulf of Aden ridge, and represents the penetration of the ridge into Afar, where it joins with the East African and Red Sea rifts (Courtillot 1980; Cochran 1981; Manighetti *et al.* 1997; Courtillot *et al.* 1999). Station ATD is located on 10–14 Ma rhyolites, and away from the main zones of rifting in the Gulf of Tadjoura (Fig. 2) (Manighetti *et al.* 1997, 1998).

The tectonic and geodynamic setting of Afar has been studied extensively (e.g. Hayward & Ebinger

From: YIRGU, G., EBINGER, C.J. & MAGUIRE, P.K.H. (eds) 2006. *The Afar Volcanic Province within the East African Rift System*. Geological Society, London, Special Publications, **259**, 239–251.
0305-8719/06/$15.00

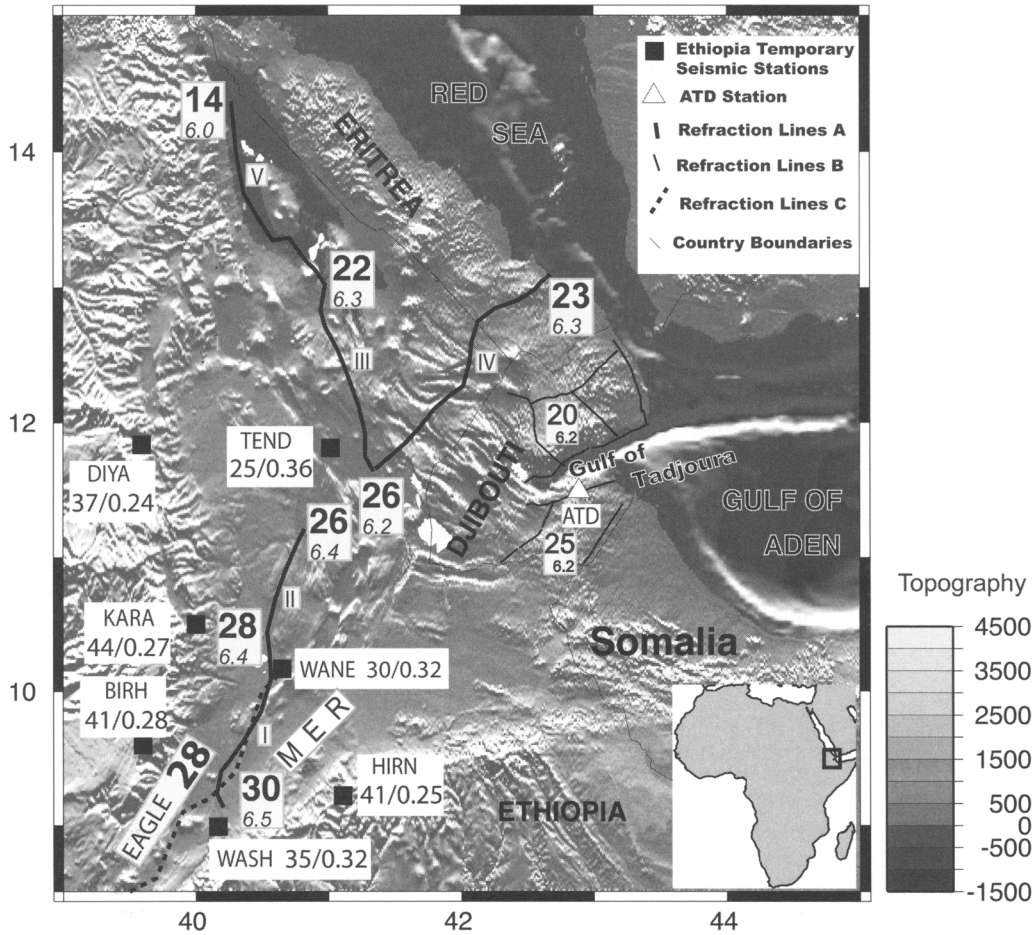

Fig. 1. Shaded relief map of the Afar region showing location of GEOSCOPE station ATD (white triangle), political boundaries (thin solid lines), temporary broadband seismic stations operated between 2000 and 2002 (black squares), and seismic refraction lines (A, Berkhemer, 1975, solid bold lines labelled I to V; B, Ruegg, 1975, medium thickness lines in Djibouti; C, EAGLE, Maguire *et al.* 2003, bold dashed line). Station names are shown in the white boxes next to seismic stations, Moho depth (in km), and crustal Poisson's ratio. Estimates of Moho depth (in km) and mean crustal V_p (in km s^{-1}) are shown in the white boxes next to seismic refraction lines, assuming the Moho is where P-wave velocities increase to $\geq$7.4 km s^{-1}.

1996; Manighetti *et al.* 1997, 1998; Acton *et al.* 2000; Ebinger & Casey 2001; Tesfaye *et al.* 2003; Audin *et al.* 2004; Wolfenden *et al.* 2005). The Red Sea and Gulf of Aden rifts began forming in the Oligocene when Arabia first separated from Africa. The western Gulf of Aden initially opened between 15 and 10 Ma and entered Afar at *c.* 5 Ma (Courtillot *et al.* 1999; Hofmann *et al.* 1997). The eruption of flood basalts in Ethiopia and Yemen occurred at about 31 Ma, concurrent with or immediately prior to the opening of the Red Sea and Gulf of Aden (d'Acremont *et al.* 2005; Wolfenden *et al.* 2005; Ukstins *et al.* 2002; Hofmann *et al.* 1997). The opening of the Main Ethiopian Rift (MER) to form the third arm of the Afar triple junction commenced around 11 Ma (Wolfenden *et al.* 2005; Chernet *et al.* 1998).

Rift models for extension in rheologically layered continental lithosphere, as found in Afar, can be grouped into two categories: (1) those invoking mechanical stretching, where strain is accommodated by large offset faults in a brittle upper crust and by ductile deformation in the lower crust; and (2) those invoking extension caused by dyke intrusion within magmatic segments (e.g. Ebinger & Casey 2001; Buck 2004; Ebinger

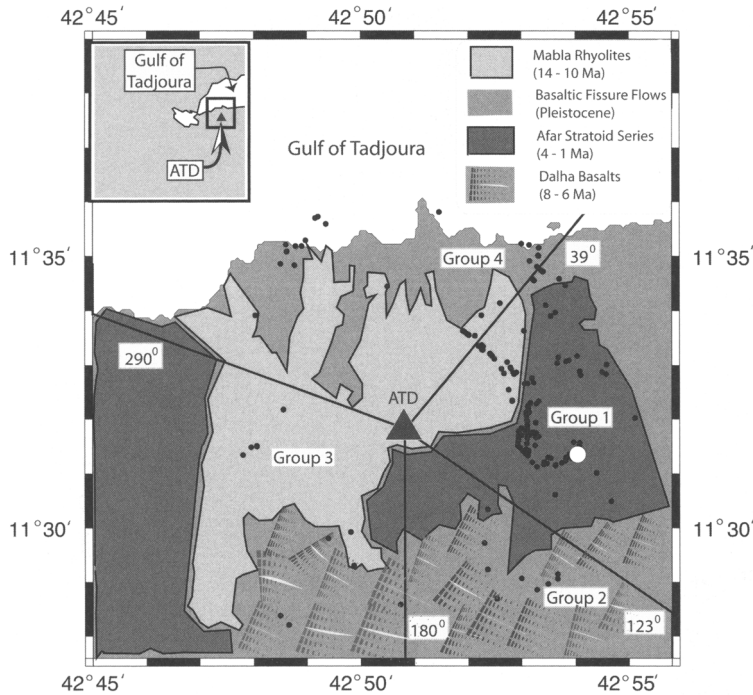

Fig. 2. Sketch map showing the geology around station ATD (solid triangle) (after Varet 1975), the distribution of Ps conversion points at a depth of 25 km (dots), and the four regions used to group receiver functions.

2005). The latter proposal has been supported for the MER and Afar by geodetic data indicating that magmatic segments accommodate >80% of the extension (Bilham *et al.* 1999), and by gravity and morphotectonic observations (Hayward & Ebinger 1996; Manighetti *et al.* 1998). A dyke intrusion model is also supported for the Afar and MER by recent shear-wave splitting studies using seismic data from the Ethiopian Afar Geoscientific Lithospheric Experiment (EAGLE) and permanent seismic stations in the region (Ayele *et al.* 2004; Kendall *et al.* 2005).

Previous studies of crustal structure in Afar

Detailed information about crustal P-wave velocity structure in Djibouti comes from the deep seismic sounding experiment of Ruegg (1975) (Fig. 1). To the south of the Gulf of Tadjoura, Ruegg (1975) reported a velocity structure consisting of five layers with P-wave velocities, from top to bottom, of 4.0 km s^{-1}, 6.4 km s^{-1}, 6.9 km s^{-1}, 7.1 km s^{-1}, and 7.4 km s^{-1}, and layer thicknesses of 3.6 km, 5.6 km, 4.6 km, 11 km and 10 km, respectively. Ruegg (1975) interpreted the Moho to be at about 10–11 km depth between layers with velocities of 6.4 km s^{-1} and 6.9 km s^{-1} (i.e. velocities of about 6.9 km s^{-1} and higher were considered to be indicative of mantle rock). Ruegg (1975) found similar structure to the north of the Gulf of Tadjoura, with increase in velocity from 7.1 km s^{-1} to 7.4 km s^{-1} occurring at a somewhat shallower depth of about 20 km.

Crustal structure has been investigated in other parts of the Afar using seismic refraction, surface wave dispersion, gravity and other geophysical data. Figure 1 summarizes Moho depths (H), crustal V_p values, and crustal Poisson's ratios reported in previous studies. Much of the information available about crustal structure in Afar comes from seismic refraction surveys conducted in the mid-1970s (Berkhemer *et al.* 1975) (lines I–V, Fig. 1). Makris & Ginzburg (1987), revising the previous interpretation of Berkhemer *et al.* (1975), reported Moho depths along refraction lines I and II of 30 km in the south and 26 km in the north. For profiles III and V, they found crustal thickness variations of 26 to 14 km, with a change in the middle of profile V from about 26 km to about 20 km. For refraction line IV, they

reported that crustal thickness thins from 26 to 23 km toward the Red Sea coast. The values of P-wave structure reported by Ruegg (1975) for the Gulf of Tadjoura region is similar to the structure reported by Makris & Ginzburg (1987) for other parts of the Afar, but the layer thicknesses are somewhat different, and also the interpretation of what velocity indicates mantle rock (i.e. how the Moho is defined). Makris & Ginzburg (1987) interpret P-wave velocities as high as 7.1–7.2 km s^{-1} as crustal velocities, and they concluded that the Moho is marked by an increase in velocity to 7.5 km s^{-1}.

Receiver functions from station ATD were modelled for crustal structure by Sandvol *et al.* (1998). They applied a grid search technique to model a receiver function stack comprised of 11 receiver functions from a limited range in backazimuth (1 event came from the west and 10 came from the east). They obtained a Moho depth of 8 km, suggesting oceanic-like crust beneath Djibouti, similar to the interpretation of crustal structure by Ruegg (1975). More recently, Dugda *et al.* (2005) analysed receiver functions from a temporary broadband station at Tendaho (TEND, Fig. 1) in central Afar, obtaining a Moho depth of 25 ± 3 km, in good agreement with estimates of crustal thickness along refraction lines II, III and IV (26 km, Fig. 1) by Makris & Ginsburg (1987).

In contrast to Moho depth, there is more uniformity in the crustal Poisson's ratios reported for the Afar. Ruegg (1975) reported a high Poisson's ratio of 0.28 to 0.33 for the Gulf of Tadjoura region, and in their global study of the continental crust, Zandt & Ammon (1995) obtained a crustal Poisson's ratio for station ATD of 0.29 ± 0.02. From an analysis of surface waves crossing Afar, Searle (1975) reported that Poisson's ratio increases from 0.25 at the surface to 0.29 at the deepest portion of the crust. Dugda *et al.* (2005) reported a high crustal Poisson's ratio of 0.36 for Tendaho (TEND, Fig. 1).

New estimates of crustal structure for Djibouti

Crustal structure has been examined in this study using data from the GEOSCOPE station ATD and two complementary methods: (1) the $H-\kappa$ receiver function stacking method; and (2) a joint inversion of receiver functions and Rayleigh wave group velocities. The first method provides estimates of Moho depth and crustal Poisson's ratio, while the second method provides information about how shear wave velocities vary with depth in the crust.

Crustal structure from $H-\kappa$ *analysis of receiver functions*

Receiver functions have been modelled for several decades using a variety of methods (e.g. Langston 1979; Taylor & Owens 1984). For this study, we have used the $H-\kappa$ stacking technique (H = Moho depth and $\kappa = V_p/V_s$) of Zhu & Kanamori (2000) because it provides robust estimates of crustal thickness and Poisson's ratio. It is well known that H and κ trade off strongly (Ammon *et al.* 1990; Zandt *et al.* 1995), and in an effort to reduce the ambiguity introduced by this trade-off, Zhu & Kanamori (2000) incorporated the later arriving crustal reverberations PpPs and PpSs + PsPs in a stacking procedure whereby the stacking itself transforms the time–domain receiver functions directly to objective function values in $H-\kappa$ parameter space. The objective function for the stacking is

$$s(H,\kappa) = \sum_{j=1}^{N} w_1 r_j(t_1) + w_2 r_j(t_2) - w_3 r_j(t_3) \quad (1)$$

where w_1, w_2, w_3 are weights, $r_j(t_i)$, $i = 1, 2, 3$ are the receiver function amplitude values at the predicted arrival times t_1, t_2, and t_3 of the Ps, PpPs, and PsPs + PpSs phases for the jth receiver function, and N is the number of receiver functions used. The $H-\kappa$ stacking algorithm is based on the premise that the weighted stack sum of the receiver function amplitudes should attain its maximum value when H and κ attain their correct values for a particular crust. By performing a grid search through H and κ parameter space, the H and κ values corresponding to the maximum value of the objective function can be determined (Zhu & Kanamori 2000). The $H-\kappa$ method provides a better estimate of Moho depth and V_p/V_s ratio than a simple stack method because it uses the correct ray parameter in the stacking of each receiver function.

Events used in this study come from distances of 30°–100° and have magnitudes greater than 5.5. Most of the events are from the east (the Indonesian and Western Pacific subduction zones), but 43 out of the 183 events come from other azimuths. For computing the receiver functions, a time-domain iterative deconvolution method (Ligorria & Ammon 1999) was used, and to evaluate the quality of the receiver functions, a least-squares misfit criterion was applied. The misfit criteria provides a measure of the closeness of the receiver functions to an ideal case, and it is calculated by using the difference between the radial component and the convolution of the vertical component with the already determined radial receiver

function. Receiver functions with a misfit of 10% and less were used in our analysis.

The receiver functions were filtered with a Gaussian pulse width of 1.6. Both radial and tangential receiver functions were examined for evidence of lateral heterogeneity in the crust and for dipping structure. Events with large amplitude tangential receiver functions were not used.

In applying the $H-\kappa$ technique, it is necessary to select weights w_1, w_2, and w_3, and a value for V_p. More weight is typically given to the phase that is most easily picked. Given a range of plausible values for average crustal V_p values for rifted continental crust (5.8–6.8 km s^{-1}; e.g. Fuchs *et al.* 1997; Prodehl *et al.* 1994 and references therein), crustal thickness can vary by almost 4 km while the V_p/V_s ratio can change by 0.02, as shown in Table 1. Thus, when estimating errors for the $H-\kappa$ method, the uncertainty in mean crustal velocity, as well as the sensitivity of the results to variations in the weights (w_1, w_2, and w_3), need to be considered.

Table 1. *Results from* H–κ *stacking of receiver functions for the different groups shown in Figure 2 for a range of plausible mean crustal* V_p

Group	V_p	Moho depth (km)	V_p/V_s	Poisson's ratio (σ)
1	**5.8**	20.7	1.84	0.29
	6.0	21.4	1.84	0.29
	6.2	22.2	1.84	0.29
	6.4	23.1	1.83	0.29
	6.6	23.8	1.83	0.29
	6.8	24.7	1.82	0.29
2	**5.8**	20.8	1.97	0.33
	6.0	21.6	1.97	0.33
	6.2	22.4	1.96	0.32
	6.4	23.3	1.95	0.32
	6.6	24.1	1.95	0.32
	6.8	25.0	1.94	0.32
3	**5.8**	21.8	1.92	0.31
	6.0	22.7	1.91	0.31
	6.2	23.4	1.91	0.31
	6.4	24.2	1.91	0.31
	6.6	25.1	1.90	0.31
	6.8	25.9	1.90	0.31
4	**5.8**	21.8	1.87	0.30
	6.0	22.5	1.87	0.30
	6.2	23.4	1.86	0.30
	6.4	24.2	1.86	0.30
	6.6	25.1	1.85	0.29
	6.8	25.9	1.85	0.29
All	**5.8**	21.1	1.89	0.31
	6.0	21.9	1.89	0.31
	6.2	22.6	1.89	0.31
	6.4	23.5	1.88	0.30
	6.6	24.4	1.87	0.30
	6.8	25.2	1.87	0.30

We used the $H-\kappa$ stacking together with a bootstrap algorithm and normally distributed values of V_p and phase weights to simultaneously find the best values of H and κ, as well as the errors associated with these values. We began by incorporating uncertainty in mean crustal velocity into error estimates for H and κ by specifying a normal distribution of V_p values so that 95% of the values selected fell between 5.9 and 6.5 km s^{-1}, with a mean value of 6.2 km s^{-1}, which is the mean crustal velocity in the refraction line near ATD (Fig. 1). For the weights (w_1, w_2 and w_3), we also used a normal distribution such that the sum of the weights add up to 1.00 but 95% of the values for w_1 fall between 0.55 and 0.65 with a mean of 0.6, for w_2 they fall between 0.25 and 0.35 with a mean value of 0.3, and for w_3 they vary between 0.05 and 0.15 with a mean value of 0.1.

Once values for V_p and the weights were selected, we then used the bootstrap algorithm of Efron & Tibshirani (1991), together with the $H-\kappa$ stacking, to estimate H and κ with statistical error bounds. While performing the $H-\kappa$ stacking, the contribution of each of the receiver functions to the determination of H and κ was also weighted based on the least squares misfit value of the receiver functions. The procedure of selecting V_p and weights from the distribution described above and then performing the $H-\kappa$ stacking with bootstrapping was repeated 200 times. After each time, new average values of H and κ and their uncertainties were computed. It was found that after repeating the procedure 50–60 times (out of 200), the error values for H and κ stabilized.

$H-\kappa$ stacking was performed on only the highest quality receiver functions (48 receiver functions spanning 10 years of data from 1993 to 2002). To examine azimuthal variation in crustal structure, the receiver functions were split into four groups from different azimuths (Fig. 2), and the stacking was performed on the receiver functions within each group. The groups were based on the clustering of the events with backazimuth, except for group 1, which we chose to be similar to the range of backazimuths represented in the receiver functions used by Sandvol *et al.* (1998). The result for group 1 is shown in Figure 3, and the results for all the groups, as well as for an $H-\kappa$ stack using all 48 receiver functions, are summarized in Table 2. The results are consistent between the various groups and give little indication of azimuthal variation in crustal structure.

For comparison with the results of Sandvol *et al.* (1998), we also computed stacks of the receiver functions by simply averaging them together (Fig. 4). Many more receiver functions were used

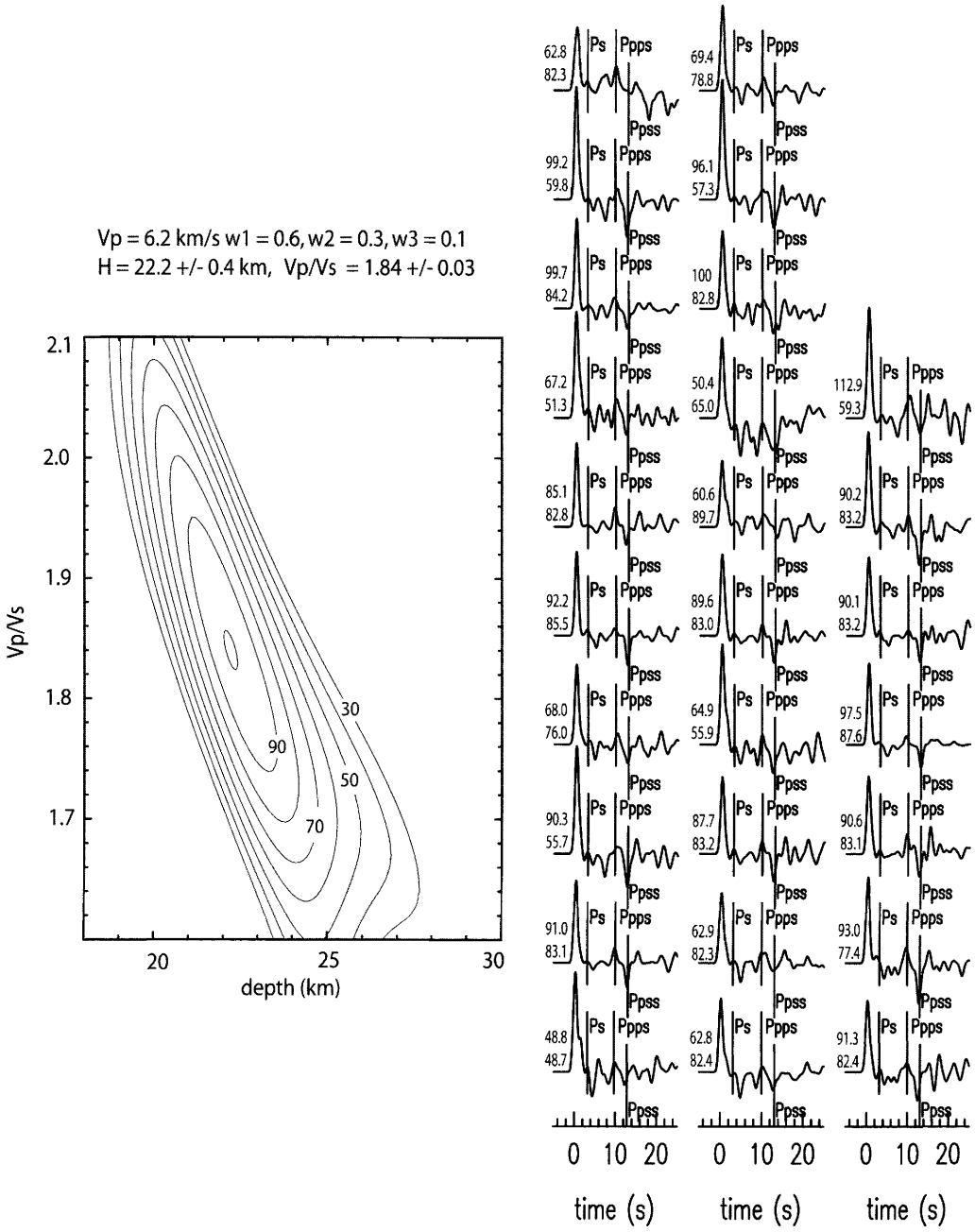

Fig. 3. $H-\kappa$ stack of receiver functions in group 1 for a mean crustal V_p of 6.2 km s^{-1}. To the left of each receiver function, the top number gives the event azimuth and the bottom number gives the event distance in degrees. Contours map out percentage values of the objective function given in the text.

Table 2. H–κ *stacking results for the groups of receiver functions shown in Figure 2 using a mean crustal* V_p *of 6.2 km* s^{-1} *and the error estimation procedure described in the text*

Group	Moho depth (km)	Depth uncertainties (+/−)	V_p/V_s	V_p/V_s uncertainties (+/−)	Poisson's ratio (σ)	No. events
1	23	1.2	1.85	0.03	0.29	27
2	23	1.7	1.95	0.05	0.32	4
3	23	2.0	1.92	0.09	0.31	9
4	24	2.4	1.86	0.10	0.30	8
All	23	1.5	1.90	0.04	0.31	48

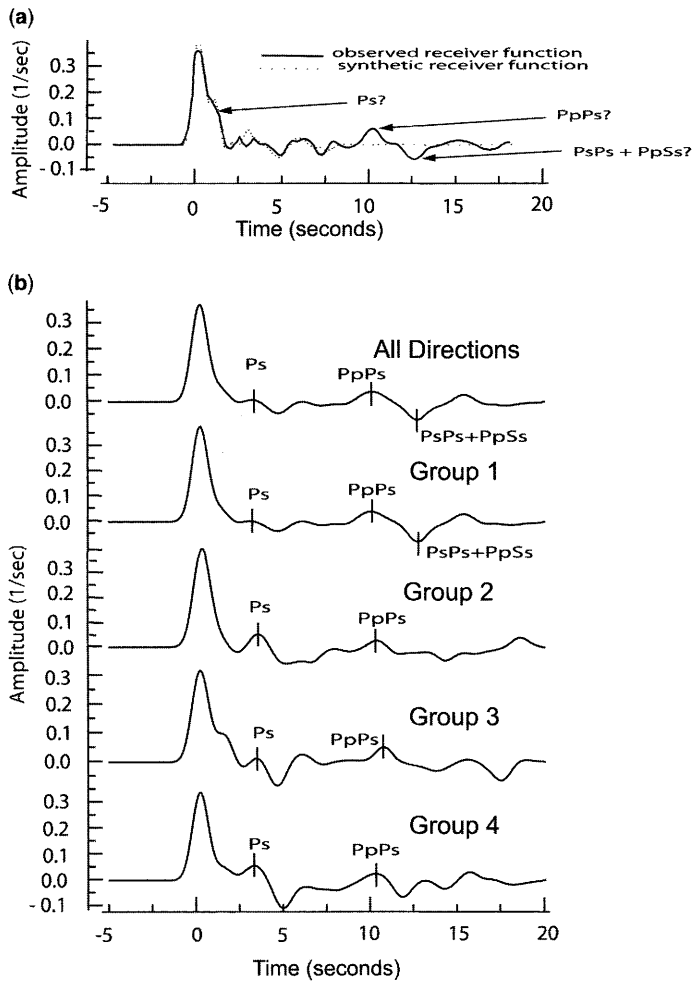

Fig. 4. (**a**) Receiver function stack and synthetic for a crustal thickness of 8 km for station ATD (redrawn from Sandvol *et al.* 1998). Crustal reverberations not interpreted by Sandvol *et al.* (1998) are labelled along with the phase they interpreted to be the Moho Ps conversion. (**b**) Simple stacks of receiver functions from this study for the different groupings shown in Figure 2.

for this (183 total), as compared to the $H-\kappa$ stacking. The Ps conversion points at 25 km depth for all 183 events are shown on Figure 2.

Crustal structure from joint inversion of receiver functions and surface wave dispersion measurements

Another approach to addressing the non-uniqueness inherent in interpreting receiver functions (besides $H-\kappa$ stacking), is to invert jointly the receiver functions with observations that constrain crustal velocities, such as surface wave dispersion measurements. Joint inversions of receiver functions and surface wave dispersion measurements have been used by many authors to obtain improved models of crustal structure (e.g. Last *et al.* 1997; Ozalaybey *et al.* 1997; Du & Foulger 1999; Julia *et al.* 2000, 2005). An advantage of this method compared to $H-\kappa$ stacking is that the inversion produces a model of shear wave velocities in the crust (in addition to Moho depth), and therefore details of crustal structure can be examined.

We used the method developed by Julia *et al.* (2000) to jointly invert the receiver functions from station ATD and surface wave group velocities. In the inversion, we used three groups of receiver functions each corresponding to a range of ray parameters from 0.04 to 0.049 (with an average value of 0.044), from 0.05 to 0.059 (with an average value of 0.056), and 0.060 to 0.069 (with an average value of 0.065) (Fig. 5). In addition, for each grouping of receiver functions, we computed and stacked two sets of receiver functions that have overlapping frequency bands: a low-frequency band of $f \leq 0.5$ Hz and a high frequency band of $f \leq 1.25$ Hz. By inverting receiver function stacks over a range of ray parameter and frequency, details of crustal structure can often be imaged, such as sharp versus gradational seismic discontinuities (Julia *et al.* 2005).

Rayleigh wave group velocities between 10 to 40 sec period were used in the inversion. The dispersion measurements come from Benoit (2005), who conducted a surface wave tomography study of eastern Africa by adding to the dispersion measurements of Pasyanos *et al.* (2001) new measurements made with data from the 2000–2002 Ethiopia broadband seismic experiment (Nyblade & Langston 2002).

The inversion was performed using two different starting velocity models to determine how sensitive the inversion results are to the starting model. In the first case (Fig. 5a), the starting model had a gradational velocity structure above 35 km over a half space. In the second case (Fig. 5b), the starting model was based on Ruegg's (1975) P-wave velocity profile converted to an S-wave model using a Poisson's ratio of 0.31.

The results from the inversions using the different starting models are nearly identical (Fig. 5), and therefore the inversion results do not appear to be influenced significantly by the starting model. The velocity models (Fig. 5) show major discontinuities at depths of about 23 km and 25 km, with a change of shear-wave velocity from about 3.75 km s^{-1} to 4.2 km s^{-1}, which we interpret to be the Moho.

To estimate the uncertainties in our model results, we followed the approach of Julia *et al.* (2005) and repeatedly performed inversions using a range of weighting parameters, constraints and Poisson's ratio. Similar to the results of Julia *et al.* (2000, 2003, 2005), by repeating the inversions for many combinations of model parameters and data, we found the uncertainties in the shear wave velocities to be about 0.1 km s^{-1} and uncertainties in the depth of discontinuities to be about 2–3 km.

Comparison of results

The results of the $H-\kappa$ stacking show little variation in crustal thickness or Poisson's ratio with backazimuth. The crustal thickness is 23 ± 1.5 km within each grouping and Poisson's ratio ranges from 0.29 to 0.32 (Tables 1 and 2). Ps conversion points shown in Fig. 2 illustrate that the receiver functions do not sample crust under the Gulf of Aden ridge. The results of the joint inversion are similar, indicating a Moho at 23 to 25 km depth.

Our results from both analyses ($H-\kappa$ stacking and joint inversion) are consistent with the seismic velocity structure given in Ruegg (1975) showing a velocity discontinuity at *c.* 24–25 km depth from 7.1 km s^{-1} to 7.4 km s^{-1}. By selecting the P to s conversion on the receiver functions at about 3 s after the P arrival as coming from the Moho, we are favouring an interpretation of crustal structure that identifies rocks with velocities as high as 7.1 km s^{-1} as crustal rock, similar to the interpretation of Makris & Ginzburg (1987) in other parts of the Afar. The Poisson's ratio of 0.31 ± 0.02 we obtained is consistent with the estimate from Ruegg (1975) of 0.28 to 0.33, as well as from Zandt & Ammon (1995) of 0.29 ± 0.02. In addition, the shear velocity structure of the crust that we obtained from our joint inversion is remarkably similar to Ruegg's (1975) model at all depths.

As reviewed earlier, Sandvol *et al.* (1998) reported a crustal thickness estimate for ATD of 8 km from analysing receiver functions. In their analysis, they used a Poisson's ratio of 0.25 and

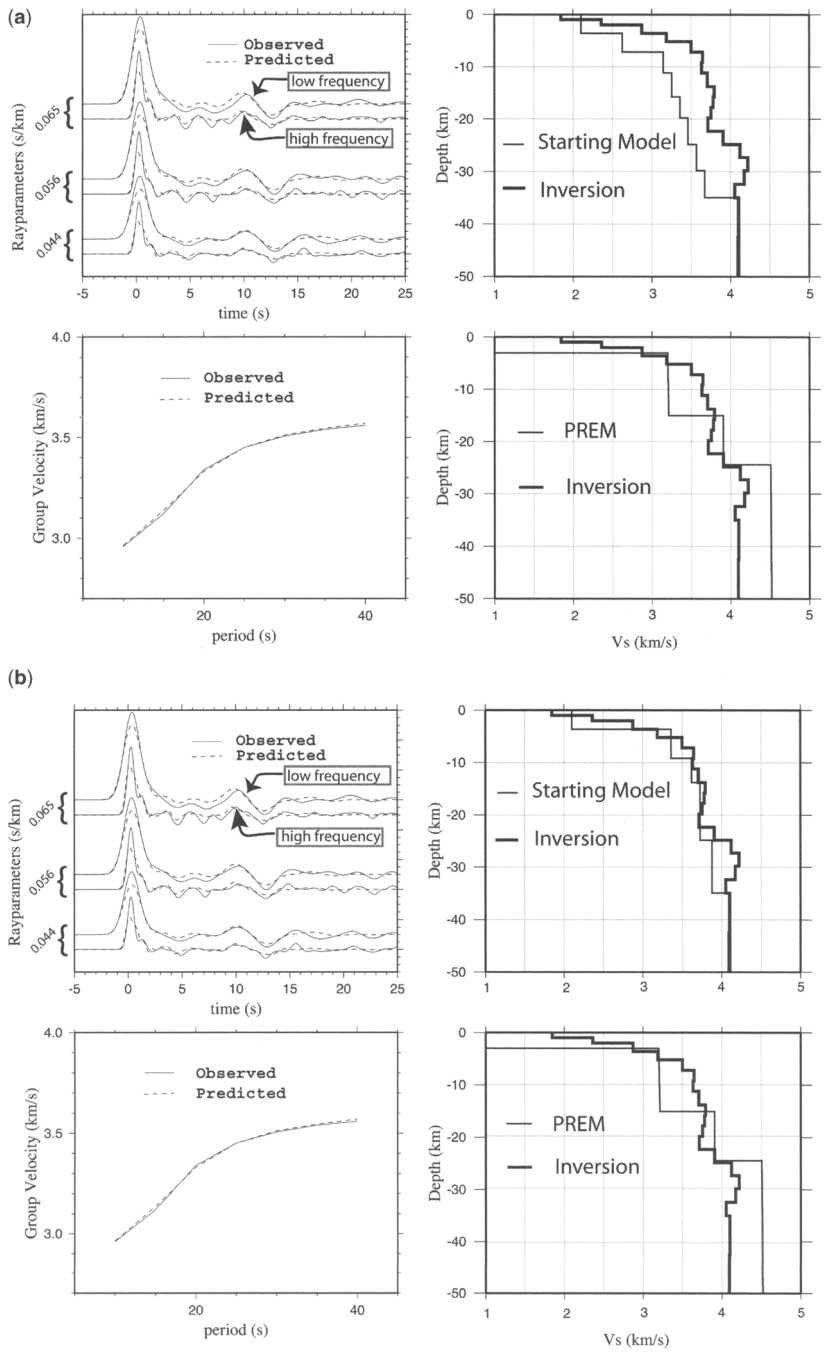

Fig. 5. Crustal shear wave velocity structure beneath station ATD from the joint inversion of receiver functions and Rayleigh wave group velocities for two different starting models: (**a**) a gradational velocity structure over a half space; and (**b**) a model based on Ruegg's (1975) P-wave velocity profile converted to an S-wave profile using a Poisson's ratio of 0.31. For both (a) and (b), upper left panel displays predicted and observed receiver functions for three different ray parameters, plus high- and low-frequency band receiver functions in each ray parameter; lower left panel shows predicted and observed surface wave group velocities; top right panel shows the starting model for the inversion and resulting model; bottom right panel displays the joint inversion result and the PREM (Preliminary Reference Earth Model; Dziewonski & Anderson 1981) model for comparison.

receiver functions from 11 events, 1 from the west and the rest from the east (backazimuths of *c.* 39° and *c.* 123°). Thus, the stack of the receiver functions they modelled primarily reflected structure beneath the area of group 1 in Fig. 2.

In comparison to Sandvol *et al.* (1998), our analysis of receiver functions is more comprehensive. We stacked many more receiver functions with good signal to noise ratios, and to check for heterogeneous structure, the receiver functions were examined in four groupings from different backazimuths, as mentioned previously. The stacked receiver functions for group 1 (Fig. 4b) show a Moho Ps phase that is much stronger than in the stack from Sandvol *et al.* (1998) (Fig. 4a). We interpret the Ps phase picked by Sandvol *et al.* (1998) to represent a shallower discontinuity, perhaps the discontinuity at about 4 km or 10 km depth seen on the refraction line from Ruegg (1975). The Ps phase that we picked as the Moho Ps conversion is not as clear on the stack used by Sandvol *et al.* (1998) as in our stack (Fig. 4b), but it is nonetheless apparent (Fig. 4a). In addition, the two reverberation phases picked by our $H-\kappa$ stacking algorithm can be seen in the stack used by Sandvol *et al.* (1998) at *c.* 10 and *c.* 12.5 seconds (Fig. 4a). The synthetic receiver function obtained by Sandvol *et al.* (1998) for their preferred crustal model does not fit the arrivals of the receiver function at those times (Fig. 4a).

Discussion

As described earlier, the Moho in the Afar has been interpreted either as an increase in velocity from about 6.4 km s^{-1} to 6.9 km s^{-1} or as an increase in velocity from about 7.1 km s^{-1} to 7.4 or 7.5 km s^{-1}. We favour the latter interpretation because a Moho at *c.* 23–25 km depth produces a Ps conversion that arrives at the time of the clearest Ps conversion on the receiver function stack for each grouping (Fig. 4b). The timing of the crustal reverberations is also well matched. In addition, the joint inversion yields a velocity structure for the crust with a clear velocity discontinuity at depths of 23–25 km (Fig. 5). Our preferred interpretation from the $H-\kappa$ stacking (Table 2) is based on a mean crustal V_p of 6.2 km s^{-1}. Results summarized in Table 1 show that even for a mean crustal V_p of 5.8 km s^{-1} (i.e. similar to the mean crustal V_p from Ruegg's model if the 7.1 km s^{-1} layer is considered to be in the mantle), the Moho depth is still around 21 km.

To the north of the Gulf of Tadjoura, Ruegg's (1975) refraction profiles show an increase in velocity from 7.1 km s^{-1} to 7.4 km s^{-1} at about 20 km depth. Hence, the crust to the north of the Gulf of Tadjoura may be somewhat thinner than to the south, but there is little indication of thin (i.e. 8–10 km thick) crust across areas of Djibouti away from the main spreading centres.

By combining our model of crustal structure beneath station ATD with the estimates of crustal structure from Makris & Ginzburg (1987), and Ruegg's (1975) velocity models for other parts of Djibouti, it appears that crustal thickness and composition may be fairly uniform across many parts of central and eastern Afar (Fig. 1). Moho depths are between 20–25 km, mean V_p is around 6.2 km s^{-1} but about 6.9–7.0 km s^{-1} below a 2–5 km-thick low-velocity layer at the surface, and Poisson's ratio is about 0.30 or higher.

What are the tectonic implications of this crustal structure for understanding the transition from continental rifting to sea-floor spreading? Mohr (1989) reviewed two plausible models for the nature of Afar crust which have different tectonic origins; (1) stretched (thinned) Precambrian continental crust modified by igneous intrusions; and (2) new igneous crust created by the addition of large volumes of mafic magma and lesser amounts of silicic magma capped by coeval flood lavas. Using estimates of crustal stretching, crustal structure and sea-floor spreading parameters for the Red Sea and Gulf of Aden basins, together with the geology of Afar indicating a region affected predominantly by fissure volcanism, Mohr (1989) argued in favour of Model 2.

Poisson's ratio is particularly diagnostic of crustal modification and was not commented on by Mohr (1989). Below the melting point of many rocks, mineralogy is the most important factor influencing Poisson's ratio (Christensen 1996), with the abundance of quartz and plagioclase feldspar having a dominant effect on the common igneous rocks. Granitic rocks have a Poisson's ratio of about 0.24, while intermediate composition rocks have values of around 0.27 and mafic rocks about 0.30 (Christensen 1996; Tarkov & Vavakin 1982).

Crustal Poisson's ratios in Afar can be used to further argue against Model 1. The Precambrian basement surrounding Afar is mostly Neoproterozoic Mozambique Belt. Dugda *et al.* (2005) have reported that average Mozambique Belt crust in eastern Africa is approximately 40 km thick, has a Poisson's ratio of about 0.25 and an average V_p of 6.5 km s^{-1}. It is very difficult to take such a crust and create the crust in Afar by simply stretching it. The resulting thinned crust would not have a sufficiently high Poisson's ratio to account for the observed Poisson's ratio in Afar of *c.* 0.30, nor would it have a sufficiently high average V_p.

Model 2 could have an appropriately high Poisson's ratio to account for the observed high ratio

found in Afar, but for this model to be viable there needs to be a reasonable explanation for how to generate the new igneous crust. One possibility is that the early Afar crust was initially oceanic in origin but was then modified by plume-generated melts from the mantle. Mohr (1978) suggested this possibility, noting that most of the anomalous crustal thickening would have occurred in the lower crustal layer (15–20 km thick in Afar compared to 4–5 km in oceanic crust), and that this amount of crustal thickening was consistent with the excessive magmatism found in Afar.

Another possibility, also proposed by Mohr (1989), is that the new igneous crust of Afar (Model 2) was generated by the intrusion of mantle-derived magmas breaking the crust. The formation of new igneous crust in this way is supported by Ebinger & Casey (2001), who suggested that in transitional rift settings extensional strain is accommodated locally within magmatic centres instead of along rift border faults. According to them, border faults (detachments) play an active controlling role in the continental break-up process during the early stages of rifting, but, in the late syn-rift stages, crustal extension results primarily from dykes intruding into the crust. Recent results from the Ethiopian Afar Geoscientific Lithosphere Experiment indicate that within the northern end of the main Ethiopian rift strain is indeed being accommodated within magmatic segments (Keir *et al.*, in press; Bendick *et al.* 2006). Consequently, the Afar crust could have been created in a similar way, with the seismic structure described above reflecting the product of extension via the addition of large volumes of intrusive rock, predominantly mafic in composition, as dykes, sills and underplate.

Conclusions

A crustal thickness of 23 $\pm$ 1.5 km and a crustal Poisson's ratio of 0.29 to 0.33 have been obtained for station ATD in Djibouti (eastern Afar) from an H–κ stacking analysis of receiver functions and a joint inversion of receiver functions and surface wave dispersion measurements. These results are consistent with the seismic velocity structure of the crust in Djibouti obtained from seismic refraction profiles (Ruegg 1975). By combining our results of crustal structure beneath station ATD with the estimates of crustal structure elsewhere in Afar, it appears that crustal thickness and composition may be fairly uniform across many parts of central and eastern Afar, with Moho depths between 20–25 km. The high Poisson's ratio and high V_p throughout most of the crust indicates a mafic composition.

The high crustal Poisson's ratio and high mean crustal V_p throughout much of Afar, as well as the crustal thickness, are not consistent with models invoking crustal formation through stretching of pre-existing Precambrian crust. Instead, we suggest that crust in Afar consists predominantly of new igneous rock emplaced as part of the extensional process. During late syn-rift stages in the main Ethiopian rift, extensional strain is accommodated within magmatic segments through dyke intrusion. In addition to dyking, sill formation and underplating associated with the magmatic centres probably combine to help form new igneous crust. The formation of the new igneous (mafic) crust in Afar could have also taken place through modification of oceanic crust that was subsequently altered by plume-derived magmas from the mantle.

We thank Chuck Ammon and Tanya Furman for helpful comments, and Cecile Doubre, Graham Stuart, Cindy Ebinger, Peter Maguire and Ian Bastow for constructive reviews. This research has been funded by the National Science Foundation (grants EAR 993093 and 0003424).

References

ACTON, G.D., TESSEMA, A., JACKSON, M. & BILHAM, R. 2000. The tectonic and geomagnetic significance of paleomagnetic observations from volcanic rocks from central Afar, Africa. *Earth and Planetary Science Letters*, **180**, 225–241.

AMMON, C.J., RANDALL, G.E. & ZANDT, G. 1990. On the nonuniqueness of receiver function inversions. *Journal of Geophysical Research*, **95**, 15303–15318.

AUDIN, L., QUIDELLEUR, X., *ET AL.* 2004. Palaeomagnetism and K–Ar and $^{40}Ar/^{39}Ar$ ages in the Ali Sabieh area (Republic of Djibouti and Ethiopia), constraints on the mechanism of Aden Ridge propagation into southeastern Afar during the last 10 Myr. *Geophysical Journal International*, **158**, 327–345.

AYELE, A., STUART, G. & KENDALL, J.-M. 2004. Insights into rifting from shear wave splitting and receiver functions: an example from Ethiopia. *Geophysical Journal International*, **157**, 354–362.

BENDICK, R., BILHAM, R., ASFAW, L. & KLEMPERER, S.L. 2006. Distributed Nubia–Somalia relative motion and dyke intrusion in the Main Ethiopian Rift. *Geophysical Journal International* (in press).

BENOIT, M. 2005. The upper mantle seismic velocity structure beneath the Arabian Shield and East Africa. PhD thesis, Department of Geosciences, Pennsylvania State University.

BERKHEMER, H., BAIER, B., *ET AL.* 1975. Deep seismic soundings in the Afar region and on the highland of Ethiopia. *In*: PILGER, A. & ROSLER, A. (eds) *Afar Depression of Ethiopia*. E. Schweizerbart, Stuttgart, 89–107.

BILHAM, R., BENDICK, R., LARSON, K., MOHR, P., BRAUN, J., TESFAYE, S. & ASFAW, L. 1999. Secular and tidal strain across the main Ethiopian rift. *Geophysical Research Letters*, **26**, 2789–2792.

BUCK, W.R. 2004. Consequences of asthenospheric variability on continental rifting. *In*: KARNER, G.D., TAYLOR, B., DRISCOLL, N. & KOHLSTEDT, D. (eds) *Rheology and Deformation of the Lithosphere at Continental Margins*. Columbia University Press, 92–137.

CHERNET, T., HART, W.K., ARONSON, J.L. & WALTER, R.C. 1998. New age constraints on the timing of volcanism and tectonism in the northern Main Ethiopian Rift–southern Afar transition zone (Ethiopia). *Journal of Volcanology and Geothermal Research*, **80**, 267–280.

CHRISTENSEN, N.I. 1996. Poisson's ratio and crustal seismology. *Journal of Geophysical Research*, **101**, 3139–3156.

COCHRAN, J.R. 1981. The Gulf of Aden; structure and evolution of a young ocean basin and continental margin. *Journal of Geophysical Research*, B, **86**, 263–287.

COURTILLOT, V. 1980. Opening of the Gulf of Aden and Afar by progressive tearing. *Physics of the Earth and Planetary Interiors*, **21**, 343–350.

COURTILLOT, V., JAUPART, C., MANIGHETTI, I., TAPPONNIER, P. & BESSE, J. 1999. On causal links between flood basalts and continental breakup. *Earth and Planetary Science Letters*, **166**, 177–195.

D'ACREMONT, E., LEROY, S., BESLIER, M.-O., BELLAHSEN, N., FOURNIER, M., ROBIN, C., MAIA, M. & GENTE, P. 2005. Structure and evolution of the eastern Gulf of Aden conjugate margins from seismic reflection data. *Geophysical Journal International*, **160**, 869–890.

DZIEWONSKI, A.M. & ANDERSON, D.L. 1981. Preliminary reference Earth model. *Physics of the Earth and Planetary Interiors*, **25**, 297–356.

DU, Z.J. & FOULGER, G.R. 1999. The crustal structure beneath the northwest fjords, Iceland, from receiver functions and surface waves. *Geophysical Journal International*, **139**, 419–432.

DUGDA, M.T., NYBLADE, A.A., JULIA, J., LANGSTON, C.A., AMMON, C.J. & SIMIYU, S. 2005. Crustal structure in Ethiopia and Kenya from receiver function analysis: implications for rift development in eastern Africa. *Journal of Geophysical Research*, **110**, B01303, doi:10.1029/2004JB003065.

EBINGER, C. 2005. The Bullerwell Lecture: Continental break-up: The East African Perspective. *Astronomy & Geophysics*, **46**, 2.16–2.21, doi:10.1111/j.1468-4004.2005.46216.x.

EBINGER, C.J. & CASEY, M. 2001. Continental breakup in magmatic provinces: An Ethiopian example. *Geology*, **29**, 527–530.

EFRON, B. & TIBSHIRANI, R. 1991. Statistical data analysis in the computer age. *Science*, **253**, 390–395.

FUCHS, K., ALTHERR, R., MULLER, B. & PRODEHL, C. (eds) 1997. Structure and dynamic processes in the lithosphere of the Afro-Arabian Rift System, Special Issue, *Tectonophysics*, **278**.

HAYWARD, N. & EBINGER, C.J. 1996. Variations in the along-axis segmentation of the Afar rift system. *Tectonics*, **15**, 244–257.

HOFMANN, C., COURTILLOT, V., FERAUD, G., ROCHETTE, P., YIRGU, G., KETEFO, E. & PIK, R. 1997. Timing of the Ethiopian flood basalt event and implications for plume birth and global change. *Nature*, **389**, 838–841.

JULIA, J., AMMON, C.J., HERRMANN, R.B. & CORREIG, A.M. 2000. Joint inversion of receiver functions and surface wave dispersion observations. *Geophysical Journal International*, **143**, 99–112.

JULIA, J., AMMON, C.J. & HERRMANN, R.B. 2003. Lithospheric structure of the Arabian Shield from the joint inversion of receiver functions and surface-wave group velocities. *Tectonophysics*, **371**, 1–21.

JULIA, J., AMMON, C.J. & NYBLADE, A.A. 2005. Evidence for mafic lower crust in Tanzania, East Africa, from joint inversion of receiver functions and Rayleigh wave dispersion velocities. *Geophysical Journal International*, **162**, 555–569.

KEIR, D., EBINGER, C., STUART, G., DALY, E. & AYELE, A. 2006. Strain accommodation by magmatism and faulting as rifting proceeds to break-up: Seismicity of the northern Ethiopian Rift. *Journal of Geophysical Research* (in press).

KENDALL, J.-M., STUART, G.W., EBINGER, C.J., BASTOW, I.D. & KEIR, D. 2005. Magma-assisted rifting in Ethiopia. *Nature*, **7022**, 146–148.

LANGSTON, C.A. 1979. Structure under Mount Rainier, Washington, inferred from teleseismic body waves. *Journal of Geophysical Research*, **84**, 4749–4762.

LAST, R.J., NYBLADE, A.A., LANGSTON, C.A. & OWENS, T.J. 1997. Crustal structure of the East African plateau from receiver functions and Rayleigh wave phase velocities. *Journal of Geophysical Research*, **102**, 24 469–24 483.

LIGORRIA, J.P. & AMMON, C.J. 1999. Iterative deconvolution and receiver-function estimation. *Bulletin of the Seismological Society of America*, **89**, 1395–1400.

MAGUIRE, P.K.H., EBINGER, C.J. *ET AL.* 2003. Geophysical Project in Ethiopia Studies Continental Breakup. *EOS Transactions, AGU*, **84**, 337, 342–343.

MAKRIS, J. & GINZBURG, A. 1987. The Afar Depression: transition between continental rifting and sea floor spreading. *Tectonophysics*, **141**, 199–214.

MANIGHETTI, I., TAPPONNIER, P., COURTILLOT, V., GRUSZOW, S. & GILLOT, P.Y. 1997. Propagation of rifting along the Arabia–Somalia plate boundary: The gulfs of Aden and Tadjoura. *Journal of Geophysical Research*, **102**, 2681–2710.

MANIGHETTI, I., TAPPONNIER, P., *ET AL.* 1998. Propagation of rifting along the Arabia-Somalia plate boundary in to Afar. *Journal of Geophysical Research*, **103**, 4947–4974.

MOHR, P. 1978. Afar. *Annual Review of Earth and Planetary Sciences*, **6**, 145–172.

MOHR, P. 1989. Nature of the crust under Afar: new igneous, not thinned continental. *Tectonophysics*, **167**, 1–11.

NYBLADE, A.A. & LANGSTON, C.A. 2002. Broadband seismic experiments probe the East African rift. *EOS Transactions AGU*, **83**, 405–408.

OZALAYBEY, S., SAVAGE, M.K., SHEEHAN, A.F., LOUIE, J.N. & BRUNE, J.N. 1997. Shear-wave velocity structure in the northern Basin and Range Province from the combined analysis of receiver functions and surface waves. *Bulletin of the Seismological Society of America*, **87**, 183–99.

PASYANOS, M.E., WALTER, W.R. & HAZLER, S.E. 2001. A surface wave dispersion study of the Middle East and North Africa for monitoring the Comprehensive Nuclear-Test-Ban Treaty. *Pure and Applied Geophysics*, **158**, 1445–1474.

PRODEHL, C., KELLER, G.R. & KHAN, M.A. 1994. Crustal and upper mantle structure of the Kenya Rift. *Tectonophysics*, **236**, 1–483.

RUEGG, J.C. 1975. Main results about the crustal and upper mantle structure of the Djibouti region (T.F.A.I.). *In*: PILGER, A. & ROSLER, A. (eds) *Afar Depression of Ethiopia*. E. Schweizerbart, Stuttgart, 120–134.

SANDVOL, E., SEBER, D., CALVERT, A. & BARAZANGI, M. 1998. Grid search modeling of receiver functions; implications for crustal structure in the Middle East and North Africa. *Journal of Geophysical Research*, **103**, 26 899–26 917.

SEARLE, R.C. 1975. The dispersion of surface waves across southern Afar. *In*: PILGER, A. & ROSLER, A. (eds) *Afar Depression of Ethiopia*. E. Schweizerbart, Stuttgart, 113–120.

TARKOV, A.P. & VAVAKIN, V.V. 1982. Poisson's ratio behavior in crystalline rocks: application to the study of the Earth's interior. *Physics of the Earth and Planetary Interiors*, **29**, 24–29.

TAYLOR, S.R. & OWENS, T.J. 1984. Frequency-domain inversion of receiver functions for crustal structure. *Earthquake Notes*, **55**, 7–12.

TESFAYE, S., HARDING, D.J. & KUSKY, T.M. 2003. Early continental breakup boundary and migration of the Afar triple junction, Ethiopia. *Bulletin of the Geological Society of America*, **115**, 1053–1067.

UKSTINS, I.A., RENNE, P.R., WOLFENDEN, E., BAKER, J., AYALEW, D. & MENZIES, M. 2002. Matching conjugate volcanic rifted margins; $^{40}Ar/^{39}Ar$ chronostratigraphy of pre- and syn-rift bimodal flood volcanism in Ethiopia and Yemen. *Earth and Planetary Science Letters*, **198**, 289–306.

VARET, J. 1975. Carte geologique de l'Afar central et septentrional au 1/500 000. Geologic map of central and northern Afar, 1:500,000. *Reunion Annuelle des Sciences de la Terre*, **3**, 370.

WOLFENDEN, E., EBINGER, C., YIRGU, G., RENNE, P.R. & KELLEY, S.P. 2005. Evolution of a volcanic rifted margin: Southern Red Sea, Ethiopia. *Geological Society of America Bulletin*, **117**, 846–864, doi: 10.1130/B25516.1.

ZANDT, G. & AMMON, C.J. 1995. Poisson's ratio of Earth's crust. *Nature*, **374**, 152–155.

ZANDT, G., MYERS, S.C. & WALLACE, T.C. 1995. Crust and mantle structure across the Basin and Range-Colorado Plateau boundary at 37 degrees N latitude and implications for Cenozoic extensional mechanism. *Journal of Geophysical Research*, **100**, 10,529–10,548.

ZHU, L. & KANAMORI, H. 2000. Moho depth variation in southern California from teleseismic receiver functions. *Journal of Geophysical Research*, **105**, 2969–2980.